Relative field line helicity of active region 11158

K. Moraitis

S. Patsourakos, A. Nindos

University of Ioannina

This research is co-financed by Greece and the European Union (European Social Fund- ESF) through the Operational Programme «Human Resources Development, Education and Lifelong Learning» in the context of the project "Reinforcement of Postdoctoral Researchers - 2nd Cycle" (MIS-5033021), implemented by the State Scholarships Foundation (IKY).

Ευρωπαϊκή Ένωση
European Social Fund

Operational Programme
Human Resources Development, Education and Lifelong Learning
Co-financed by Greece and the European Union

ΕΣΠΑ
2014-2020
ανάπτυξη - εργασία - αλληλεγγύη

Outline

- Introduction – Magnetic helicity
- Field line helicity
- Active Region 11158
- Application to AR 11158
- Conclusions

Magnetic helicity

- Magnetic helicity is a geometrical measure of the twist and writhe of the magnetic field lines, and of the amount of flux linkages between pairs of lines (Gauss linking number)
- Mathematically, it is defined as

$$H = \int_V \boldsymbol{A} \cdot \boldsymbol{B} \, dV$$

$$\boldsymbol{B} = \nabla \times \boldsymbol{A}$$

- Signed scalar quantity (right (+), or left (-) handed)
- Units of magnetic flux squared (SI: Wb^2, cgs: Mx^2)

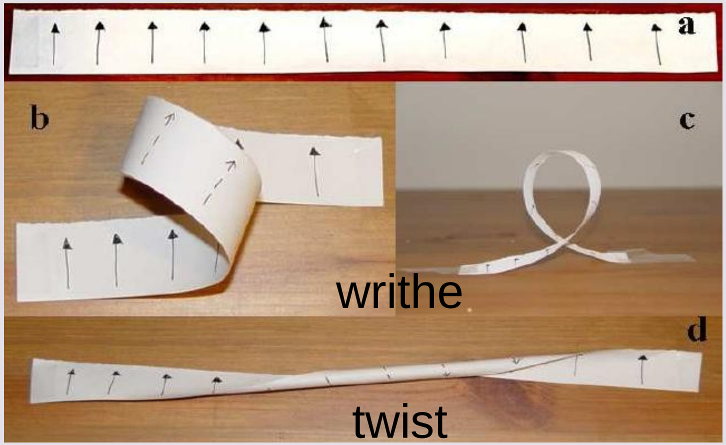

$$H = (Tw + Wr)\,\Phi^2$$

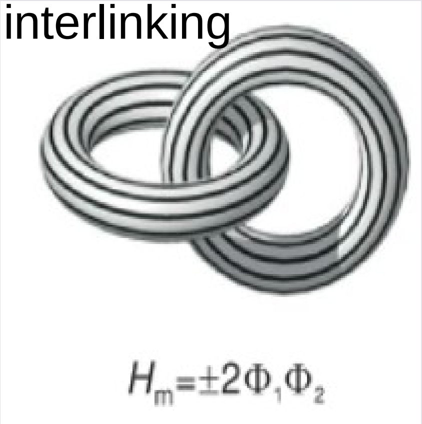

Magnetic helicity properties

- Conserved in ideal MHD (Woltjer 1958), along with energy and cross helicity

$$\frac{dH_m}{dt} = \int_{\partial\mathcal{V}} \left(\mathbf{A} \times \frac{\partial \mathbf{A}}{\partial t}\right) \cdot \mathrm{d}\mathbf{S} - 2\int_{\partial\mathcal{V}} (\mathbf{E} \times \mathbf{A}) \cdot \mathrm{d}\mathbf{S} - 2\int_{\mathcal{V}} \mathbf{E} \cdot \mathbf{B} \;\, \mathrm{d}\mathcal{V}$$

- Topological invariant; links cannot change by ‘frozen’ magnetic field lines
- Even in resistive MHD (reconnection), helicity is approximately conserved (Taylor 1975; Pariat et al. 2015)
- Coronal mass ejections are caused by the need to expel the excess helicity accumulated in the corona (Rust 1994)
- Linear force-free field = the minimum energy field for given helicity (Woltjer 1958)

Relative magnetic helicity

magnetic helicity

$$H=\int_V \boldsymbol{A}\cdot\boldsymbol{B}\,dV$$

under the gauge transformation

$$\boldsymbol{A}'=\boldsymbol{A}+\nabla\xi$$

becomes

$$H'=H+\oint\xi\,\boldsymbol{B}\cdot d\,\boldsymbol{S}$$

gauge independent for closed ***B***

$$\hat{n}\cdot\boldsymbol{B}\big|_{\partial V}=0$$

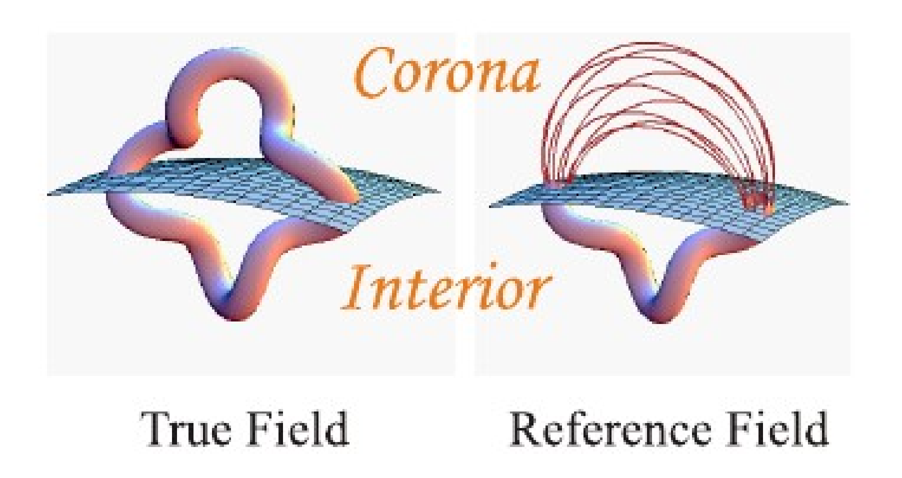

Berger & Field 1984; Finn & Antonsen 1985

relative magnetic helicity

$$H_r=\int_V(\mathbf{A}+\mathbf{A}_{\mathrm{p}})\cdot(\mathbf{B}-\mathbf{B}_{\mathrm{p}})\,dV$$

gauge independent for closed (and solenoidal) $\boldsymbol{B}-\boldsymbol{B}_p$

$$\hat{n}\cdot\boldsymbol{B}\big|_{\partial V}=\hat{n}\cdot\boldsymbol{B}_p\big|_{\partial V}$$

- ∂V: the whole boundary
- reference field=potential
- no current $\rightarrow$ no helicity
- single number characterizes whole volume

Can we define a helicity density?

and not ***A.B*** ?

$$H = \int_V \boldsymbol{A} \cdot \boldsymbol{B} \, dV$$

$$\neq$$

$$m = \int_V \rho \, dV$$

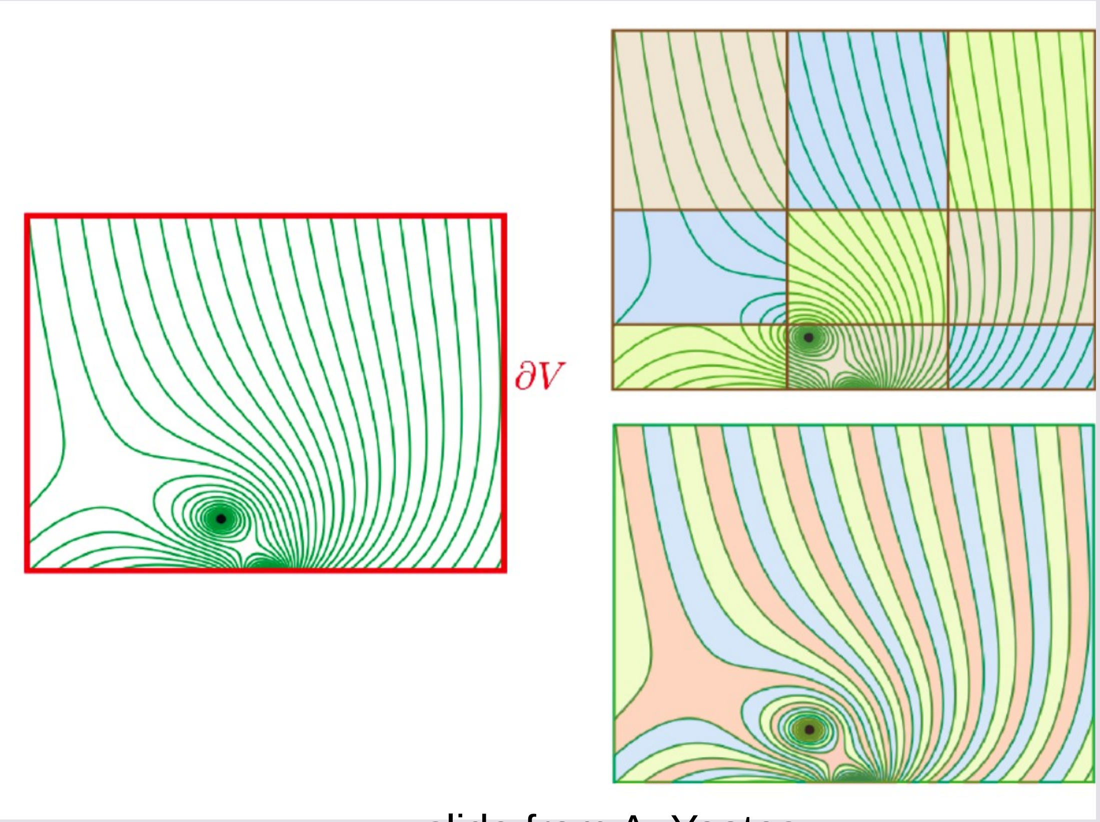

slide from A. Yeates

Field line helicity

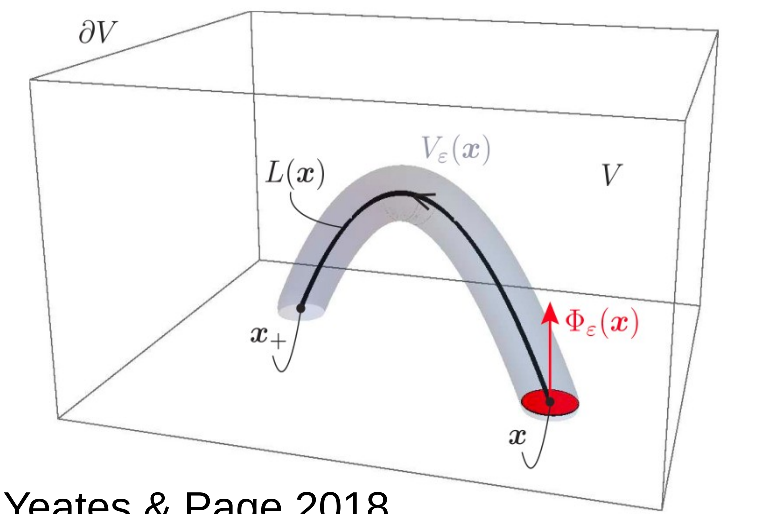

Yeates & Page 2018

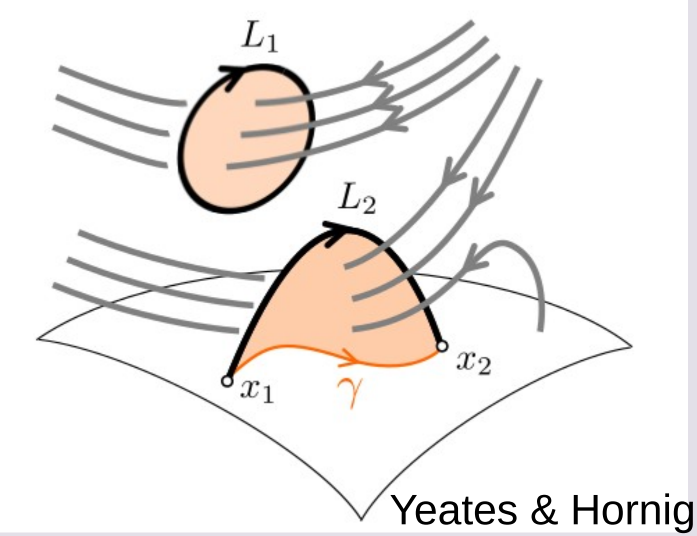

Yeates & Hornig 2016

$$\begin{aligned}\mathcal{A}(C) &= \lim_{\epsilon\to 0}\left(\frac{1}{\Phi_\epsilon}\int_{V_\epsilon}\mathbf{A}\cdot\mathbf{B}\,\mathrm{d}V\right) \\ &= \lim_{\epsilon\to 0}\left(\frac{1}{\Phi_\epsilon}\int_{V_\epsilon}(\mathbf{A}\cdot\mathrm{d}\boldsymbol{l})\,(\mathbf{B}\cdot\mathrm{d}\boldsymbol{S})\right) \\ &= \int_C \mathbf{A}\cdot\mathrm{d}\boldsymbol{l}\end{aligned}$$

$$\mathrm{d}V = \mathrm{d}\boldsymbol{S}\cdot\mathrm{d}\boldsymbol{l}$$

+ Magnetic helicity reduces to a surface integral along the boundary

$$H = \int_{\partial V}\mathcal{A}\,d\Phi$$

- FLH is gauge-dependent

Relative field line helicity

$$H_r = \int_V (\mathbf{A} + \mathbf{A}_\mathrm{p}) \cdot (\mathbf{B} - \mathbf{B}_\mathrm{p})\, dV$$

$$H_r = \int_{\partial V} \mathcal{A}_r \,\mathrm{d}\Phi$$

$$\mathcal{A}_r^+ = \int_{\alpha_+}^{\alpha_-} (\mathbf{A} + \mathbf{A}_\mathrm{p}) \cdot \mathrm{d}\boldsymbol{l} - \int_{\alpha_+}^{\alpha_{p-}} (\mathbf{A} + \mathbf{A}_\mathrm{p}) \cdot \mathrm{d}\boldsymbol{l}_\mathrm{p}$$

$$\mathcal{A}_r^- = \int_{\alpha_+}^{\alpha_-} (\mathbf{A} + \mathbf{A}_\mathrm{p}) \cdot \mathrm{d}\boldsymbol{l} - \int_{\alpha_{p+}}^{\alpha_-} (\mathbf{A} + \mathbf{A}_\mathrm{p}) \cdot \mathrm{d}\boldsymbol{l}_\mathrm{p}$$

$$\partial V^\pm = \{\mathbf{x} \in \partial V : \hat{n} \cdot \mathbf{B}(\mathbf{x}) \lessgtr 0\}$$

$$\mathcal{A}_r^0 = \frac{1}{2}\left(\mathcal{A}_r^+ + \mathcal{A}_r^-\right)$$

Moraitis et al. 2019

$$\mathcal{A}_r^{\mathrm{YP},+} = \int_{\alpha_+}^{\alpha_-} \mathbf{A} \cdot \mathrm{d}\boldsymbol{l} - \int_{\alpha_+}^{\alpha_{p-}} \mathbf{A}_\mathrm{p} \cdot \mathrm{d}\boldsymbol{l}_\mathrm{p}$$

Yeates & Page 2018

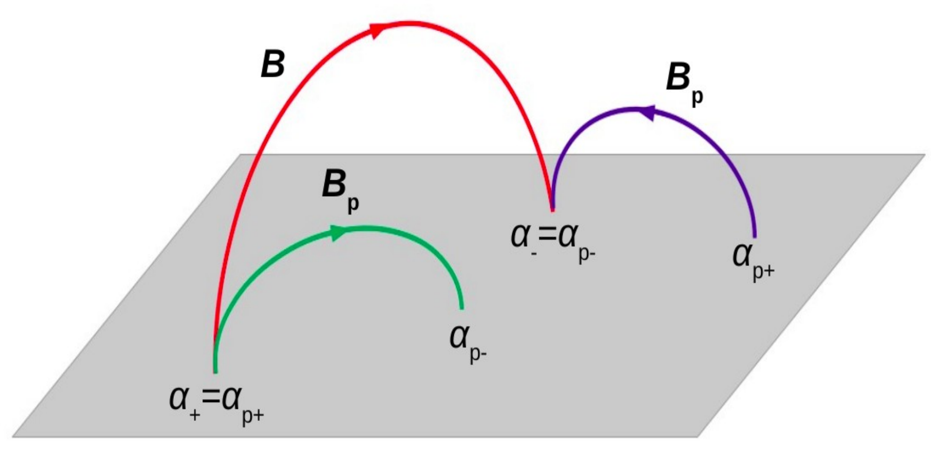

All expressions are gauge-dependent

Computing RFLH

Input: 3D magnetic field ***B*** in the volume

Instantaneous finite-volume computation

$$H_r = \int_V (\mathbf{A} + \mathbf{A}_\mathrm{p}) \cdot (\mathbf{B} - \mathbf{B}_\mathrm{p})\, dV$$

$$H_r = \int_{\partial V^+} \mathcal{A}_r^+ \, d\Phi$$

$$\mathcal{A}_r^+ = \int_{\alpha_+}^{\alpha_-} (\mathbf{A} + \mathbf{A}_\mathrm{p}) \cdot dl - \int_{\alpha_+}^{\alpha_{p-}} (\mathbf{A} + \mathbf{A}_\mathrm{p}) \cdot dl_\mathrm{p}$$

1. given ***B*** find $\boldsymbol{B}_\mathrm{p}$
2. given ***B***, $\boldsymbol{B}_\mathrm{p}$ find ***A***, $\boldsymbol{A}_\mathrm{p}$
3. given ***B***, $\boldsymbol{B}_\mathrm{p}$, ***A***, $\boldsymbol{A}_\mathrm{p}$ find RFLH

Computing RFLH

Step 1 – Potential field calculation

$$\mathbf{B}_\mathrm{p} = \nabla\Phi$$
$$\hat{n}\cdot\mathbf{B}_\mathrm{p}|_{\partial V} = \hat{n}\cdot\mathbf{B}|_{\partial V}$$

$\rightarrow$

$$\nabla^2\Phi = 0$$
$$\left.\frac{\partial\Phi}{\partial\hat{n}}\right|_{\partial V} = \hat{n}\cdot\mathbf{B}|_{\partial V}$$

solution of Laplace's eq. under Neumann BCs

Step 2 – Vector potentials calculation

invert $\mathbf{B} = \nabla\times\mathbf{A}$ using DeVore (2000) gauge $\hat{\mathbf{z}}\cdot\mathbf{A} = 0$

$$\mathbf{A}(x,y,z) = \boldsymbol{\alpha}(x,y) + \hat{\mathbf{z}}\times\int_{z_0}^{z}\mathrm{d}z'\,\mathbf{B}(x,y,z')$$

$$\nabla_\perp\times\boldsymbol{\alpha} = B_z(x,y,z_0)$$

- simple gauge (DVS)
- Coulomb gauge (DVC) $\nabla_\perp\cdot\boldsymbol{\alpha} = 0$

Step 3 – Field line integrations

modification of QSL Squasher code (Tassev & Savcheva 2016) which uses a fast and robust adaptive RK C++ routine

- same method for both field line integrations
- addition of one more equation

$$\frac{\mathrm{d}h}{\mathrm{d}s} = \frac{(\mathbf{A}+\mathbf{A}_\mathrm{p})\cdot\mathbf{B}}{B}$$

  to the system solved by the code
- user-supplied starting points instead of automatically determined

Field line helicity applications

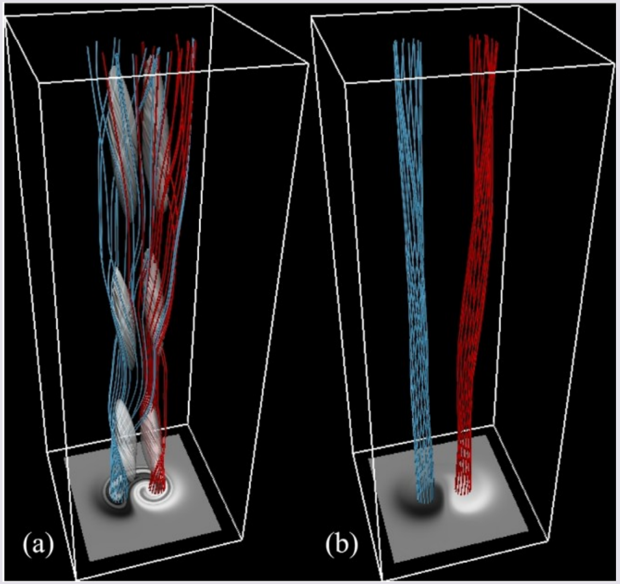

Yeates & Hornig 2013, 2014
Unique topological characterization of magnetic braids
Russel et al. 2015
FLH evolution during magnetic reconnection

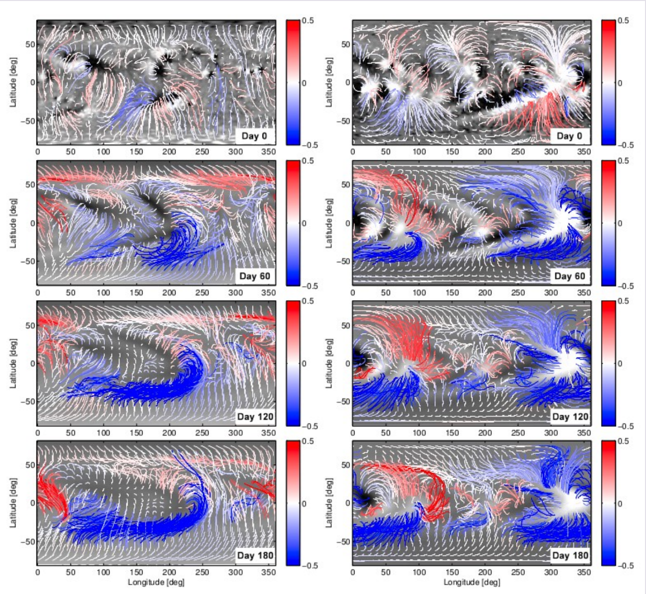

Yeates & Hornig 2016
Non-uniform distribution of FLH, highly concentrated in twisted flux ropes

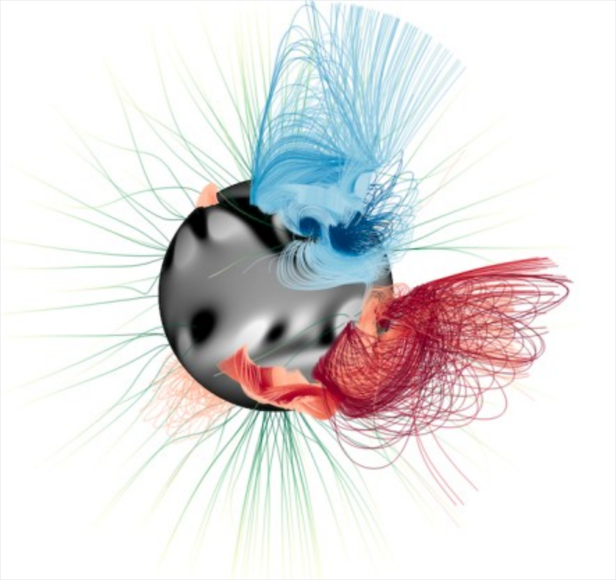

Lowder & Yeates 2017
Flux rope identification

RFLH applications

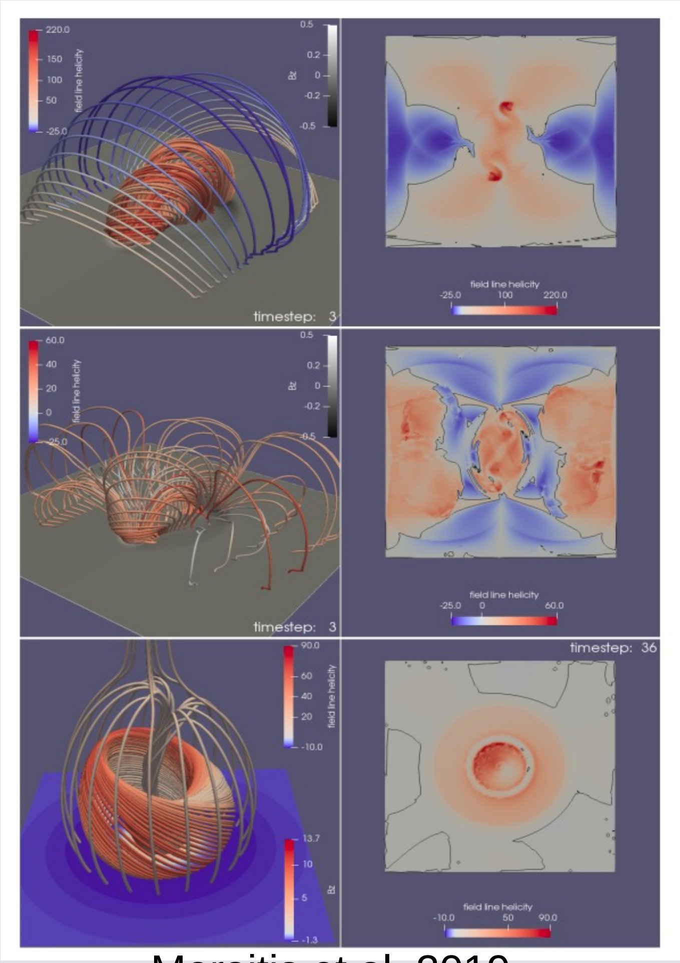

Moraitis et al. 2019

MHD simulations:
non-eruptive/eruptive flux emergence
Leake et al. 2013, 2014
coronal jet formation
Pariat et al. 2009

Semi-analytic
FF field of
Low & Lou (1990)

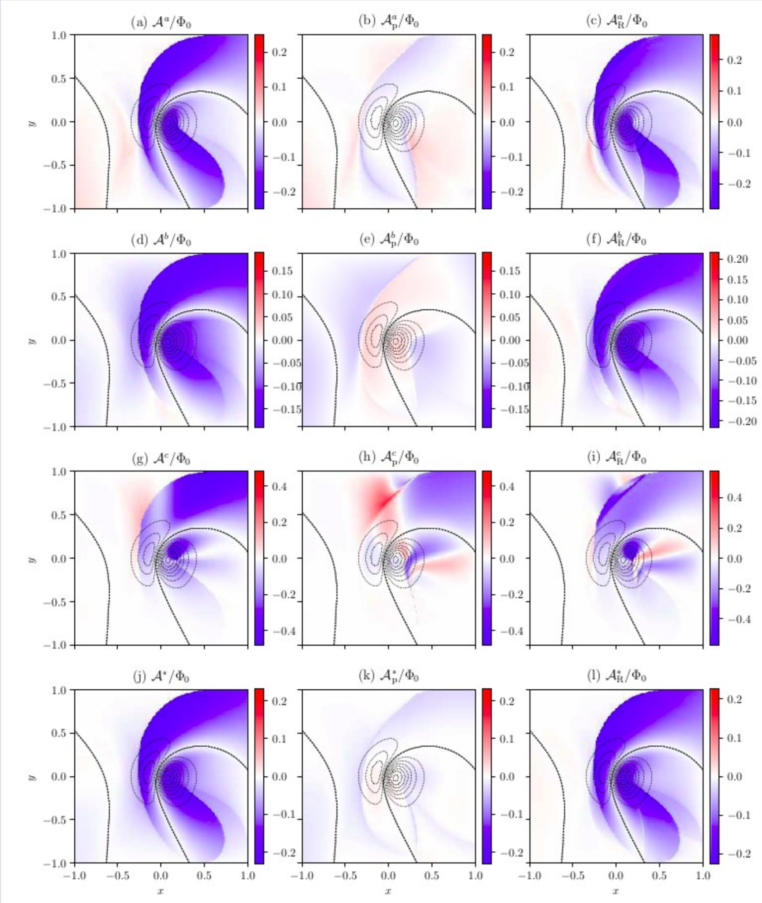

Yeates & Page 2018

Active Region 11158

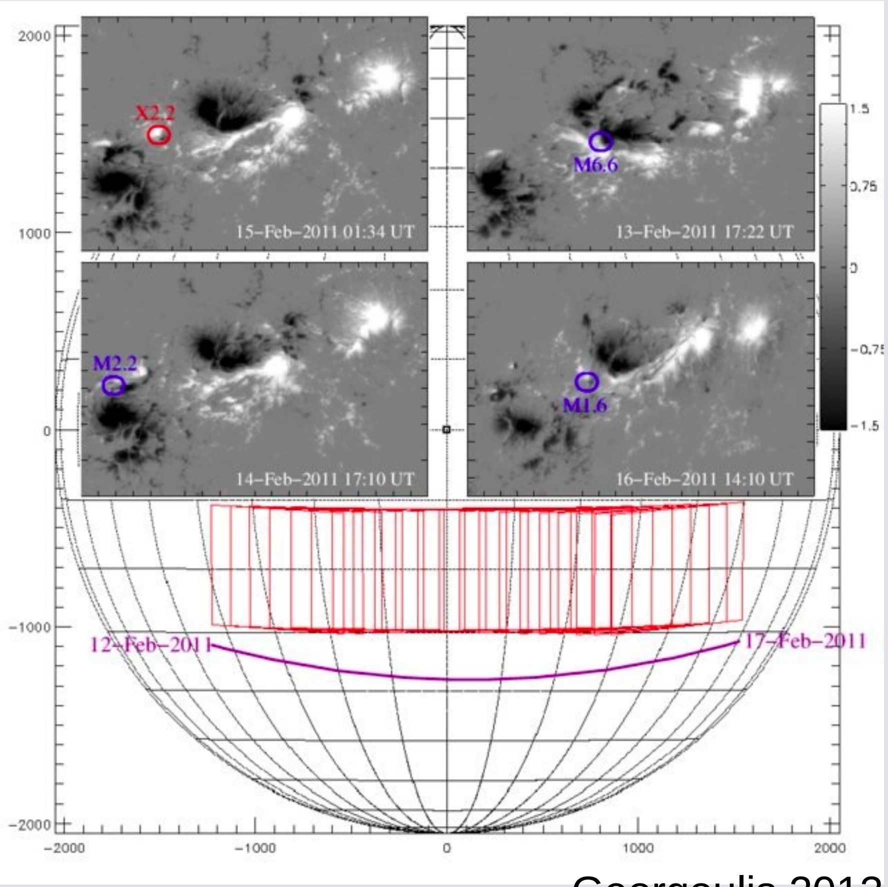

Georgoulis 2013

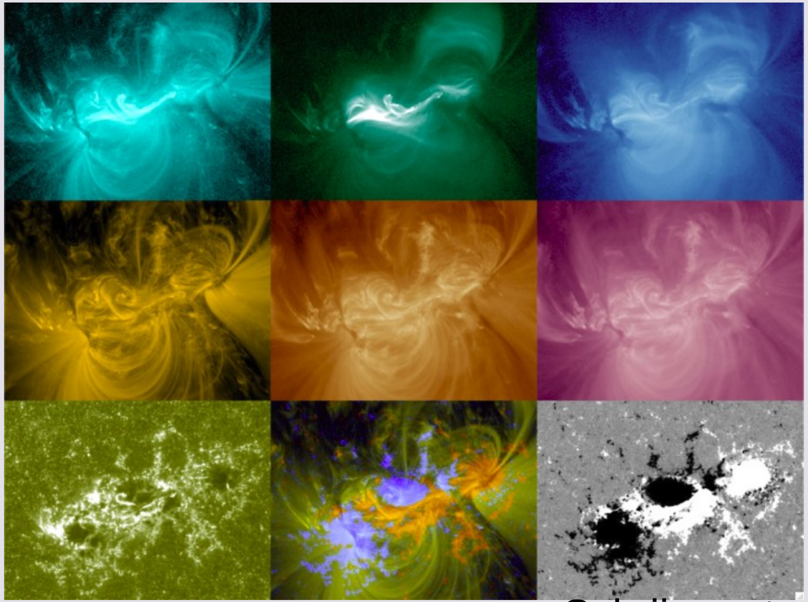

Schrijver et al. 2011

1st SDO/HMI AR
12-17 Feb 2011
3 M-class flares +
an X2.2, all eruptive

AR 11158 coronal magnetic field modeling

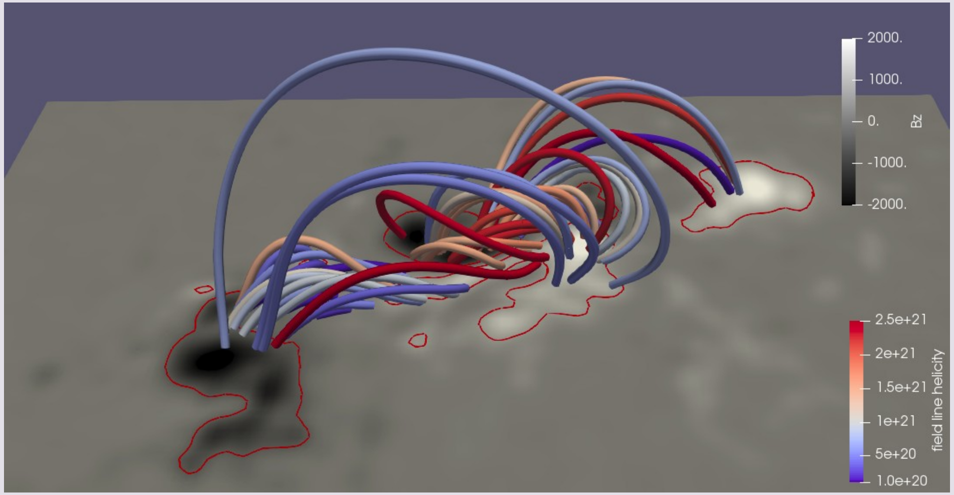

15 Feb 2011, 01:11 UT

NLFF extrapolation (Thalmann et al. 2019)
215 Mm x 130 Mm x 185 Mm
148 x 92 x 128 grid points
resolution 2’’ per pixel
12-16 Feb 2011
1 hr cadence + 12 min around the M6.6 and the X2.2 flares
115 snapshots in total

High-quality reconstruction
f_i=2.2 x 10^{-4}
E_{div}/E=0.006
essential for reliable helicity values (Valori et al. 2016)

RFLH morphology

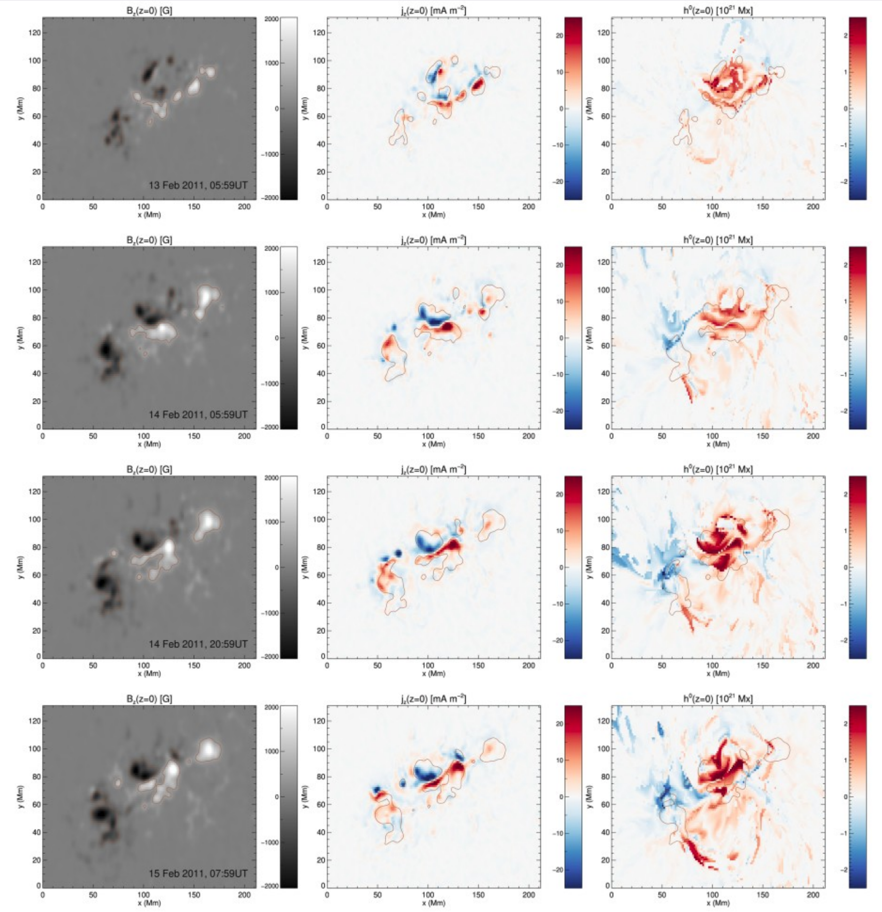

RFLH tests

$$H_r = \int_V (\mathbf{A} + \mathbf{A}_\mathrm{p}) \cdot (\mathbf{B} - \mathbf{B}_\mathrm{p})\, dV$$

$$H_r = \int_{\partial V} \mathcal{A}_r^0 \,\mathrm{d}\Phi$$

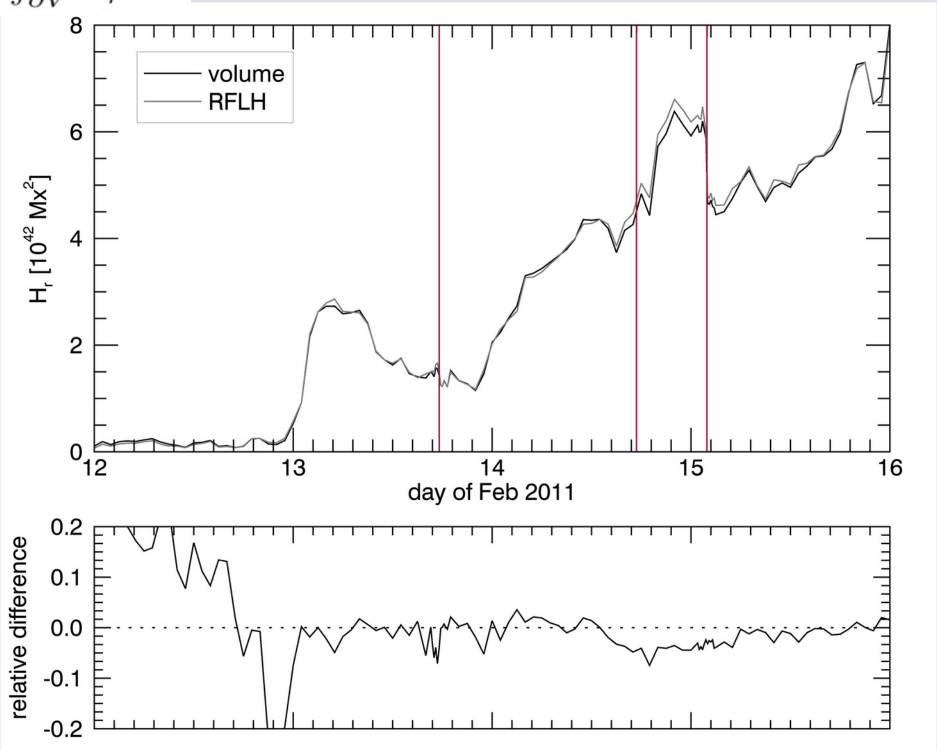

gauge dependency

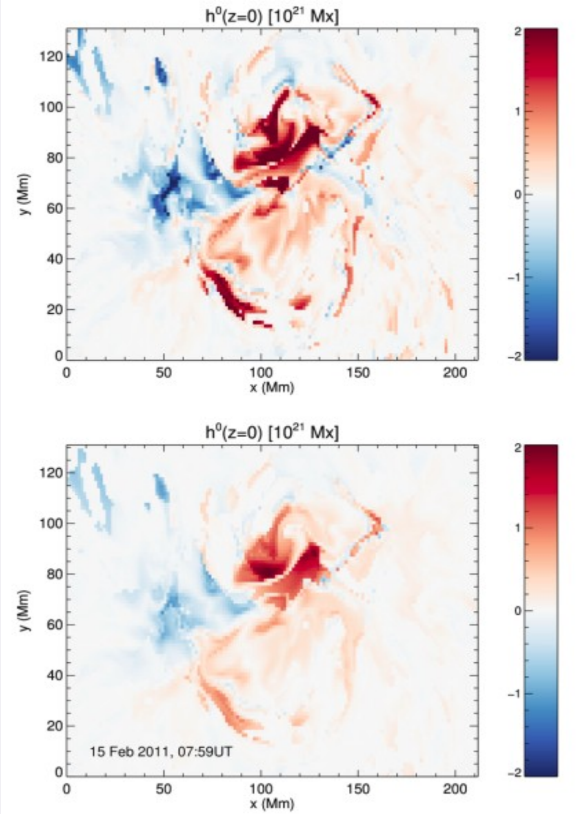

ROIs identification

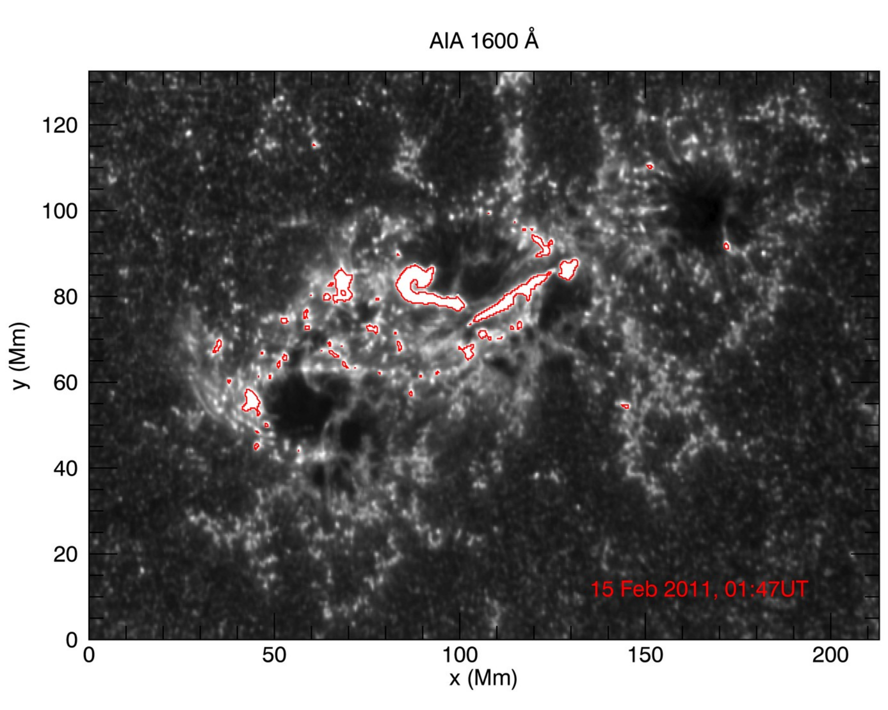

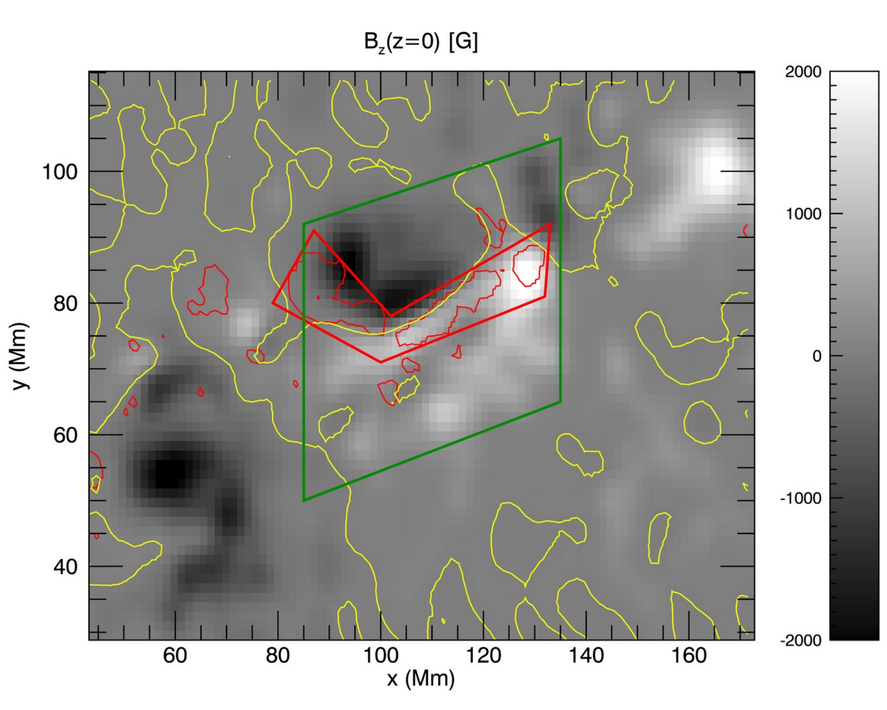

RFLH morphology around the X2.2 flare

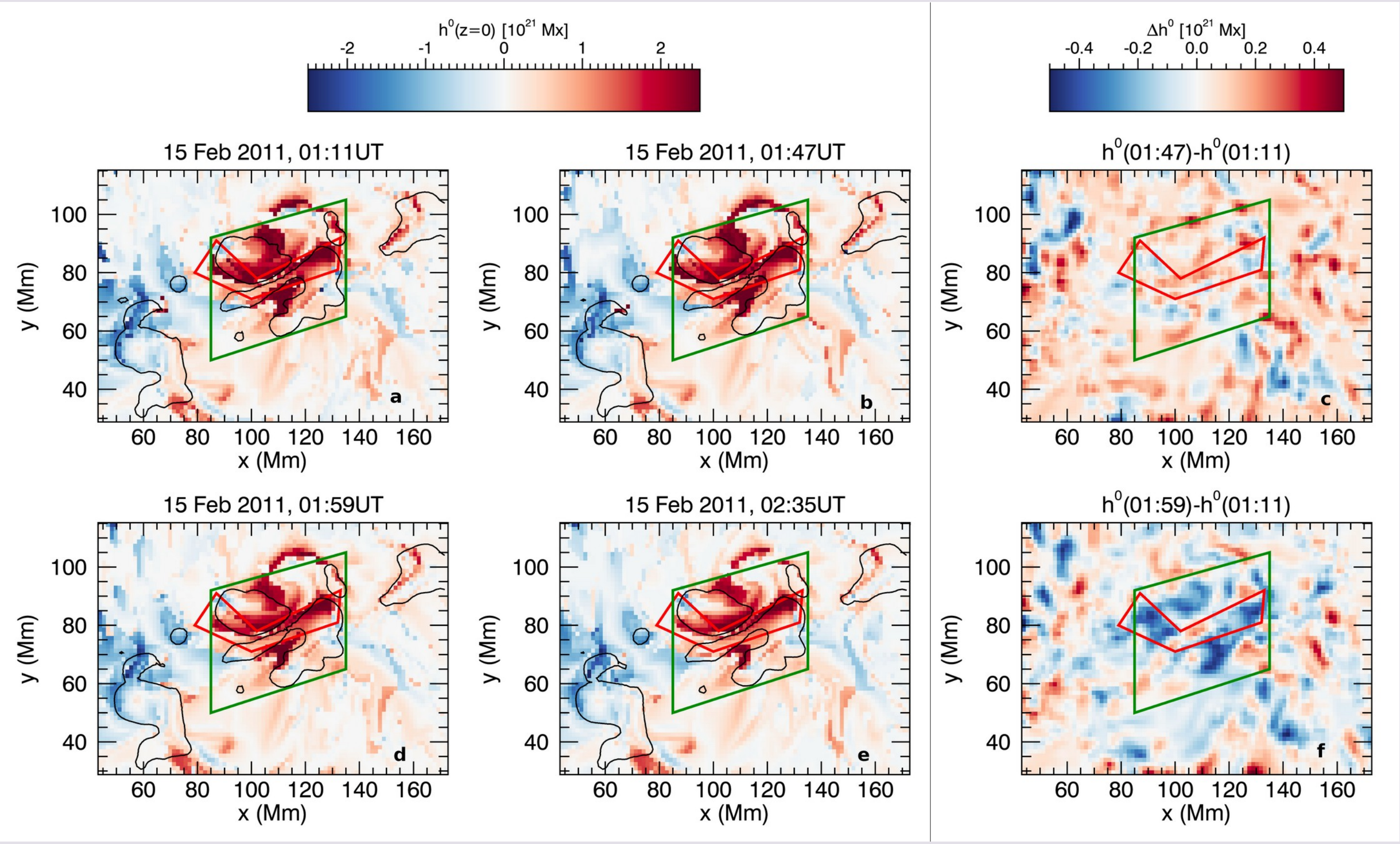

Flare-related changes during the X2.2 flare

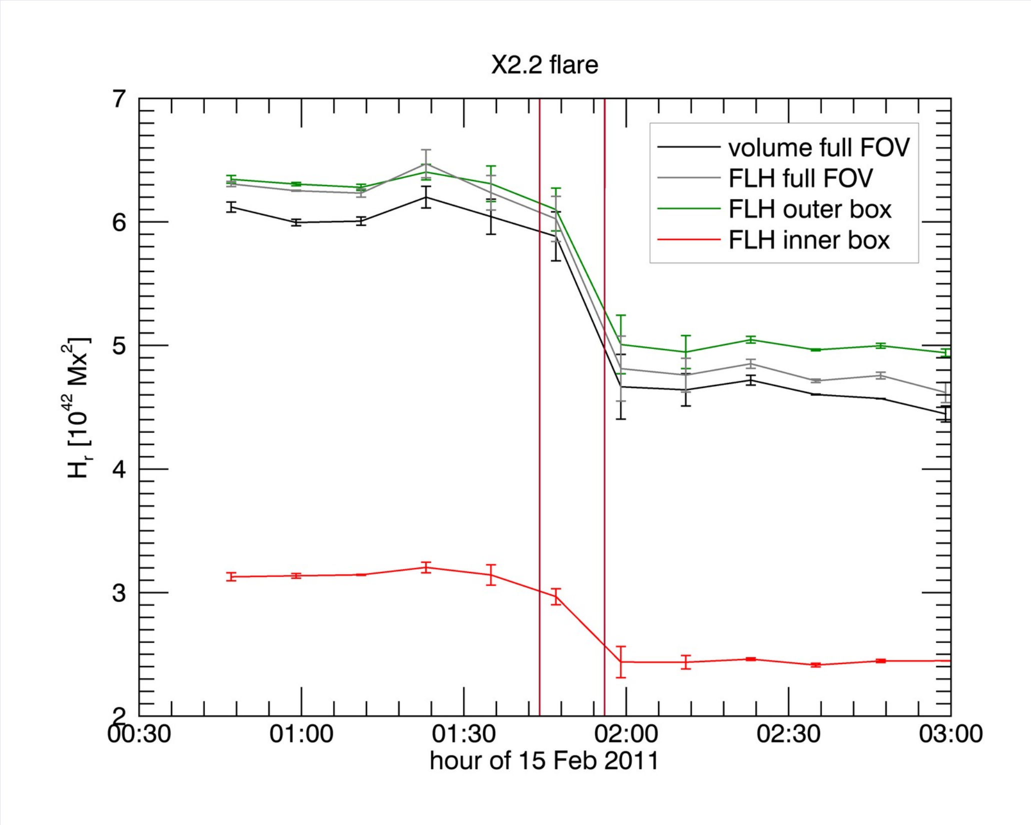

- Volume + FLH agree to <5%
- Green box contains almost the same amount of helicity as whole FOV, more before the flare
- All curves drop by 20-25% (beyond errors) during flare, ~1.5×10^{42} Mx^2
- Red box contains half helicity, and drops by 7×10^{41} Mx^2
- Unfortunately, no relation with the detected ICME possible, 2×10^{41} Mx^2

Conclusions

- Relative field line helicity is a good proxy for the density of relative helicity
- First application of RFLH in a solar active region – Moraitis, Patsourakos & Nindos 2021, Astronomy & Astrophysics, 649, A107
- RFLH has important potential in highlighting locations of intense helicity
- Main disadvantage of RFLH is its gauge dependence
- With RFLH we can compute the helicity, or the helicity difference between two instances, in an arbitrarily-shaped photospheric ROI